Predicting SQL Query Execution Time with a Cost Model for Spark Platform

Aleksey Burdakov[1], Viktoria Proletarskaya[1], Andrey Ploutenko[2], Oleg Ermakov[1] and Uriy Grigorev[1]
[1]*Informatics and Control Systems, Bauman Moscow State Technical University, Moscow, Russia*
[2]*Mathematics and Informatics, Amur State University, Blagoveschensk, Russia*

Keywords: SQL, Apache Spark, Bloom Filter, TPC-H Test, Big Data, Cost Model.

Abstract: The paper proposes a cost model for predicting query execution time in a distributed parallel system requiring time estimation. The estimation is paramount for running a DaaS environment or building an optimal query execution plan. It represents a SQL query with nested stars. Each star includes dimension tables, a fact table, and a Bloom filter. Bloom filters can substantially reduce network traffic for the Shuffle phase and cut join time for the Reduce stage of query execution in Spark. We propose an algorithm for generating a query implementation program. The developed model was calibrated and its adequacy evaluated (50 points). The obtained coefficient of determination R^2=0.966 demonstrates a good model accuracy even with non-precise intermediate table cardinalities. 77% of points for the modelling time over 10 seconds have modelling error Δ<30%. Theoretical model evaluation supports the modelling and experimental results for large databases.

1 INTRODUCTION

Database query execution forecasting has always been an important task. This task has become even more valuable in the Database as a Service (DaaS) (Wu, 2013) context. A DaaS provider has to manage infrastructure costs, and Service Level Agreements (SLA). Query execution estimates can help system management (Wu, 2013) in:

1. Access Control: by evaluating whether a query can be executed (Tozer et al., 2010; Xiong et al., 2011).
2. Query Planning: by planning for delays and query execution time limits (Chi et al., 2011; Guirguis et al., 2009).
3. Progress Monitoring: by eliminating abandoned large queries that overload the system (Mishra et al., 2009).
4. System Calibration: by designing and tuning the system based on query execution time dependency on the hardware resources (Wasserman et al., 2004).

There are two major approaches for database query execution time forecasting:

1) Machine Learning (ML) methods that look at the DBMS as a black box and attempt to build a prognostic model (Tozer et al., 2010; Xiong et al., 2011; Akdere et al., 2012; Ganapathi et al., 2009),

2) Cost Models (Wu, 2013; Leis et al., 2015).

ML methods give a significant error as shown in (Wu, 2013). This is potentially caused by assumed test and model training queries similarity. This assumption is not correct for real dynamic database loads. In this case, the query execution plans can differ dramatically and the time changes radically.

Using exact table row counts in cost models allows building a precise linear correlation between query execution time and query cost for real databases (Leis et al., 2015). Model parameters calibration and utilization of exact row counts give the lowest query execution time error for the cost model (Wu, 2013).

Sources (Wu, 2013; Leis et al., 2015) consider the predictive cost model only for relational databases. At the same time MapReduce (Dean et al., 2004) is widely used to implement big database queries. It assumes a parallel execution of the queries to data fragments distributed over many nodes (workers). Several data access platforms use this technology (Mistrík et al., 2017; Armbrust et al., 2015). The source (Armbrust et al., 2015) shows that Apache Spark SQL has advantages. The original query is split into tasks and tasks into stages. Each stage usually includes Map and Reduce execution.

Burdakov, A., Proletarskaya, V., Ploutenko, A., Ermakov, O. and Grigorev, U.
Predicting SQL Query Execution Time with a Cost Model for Spark Platform.
DOI: 10.5220/0009396202790287
In *Proceedings of the 5th International Conference on Internet of Things, Big Data and Security (IoTBDS 2020)*, pages 279-287
ISBN: 978-989-758-426-8
Copyright © 2020 by SCITEPRESS – Science and Technology Publications, Lda. All rights reserved

The paper discusses a new cost model for SQL query execution time prediction for the Spark platform. This model accounts for Bloom filter and small tables duplication over the nodes. These aspects significantly reduce the original query execution time (Burdakov et al., 2019). The developed model also helps in making an optimal SQL query execution plan in a distributed environment.

In Paragraph 2, we illustrate how the source queries can be represented as subqueries and where you can connect and use Bloom filters. Then we extend this approach to the general case (Table 1). Details of the developed method for SQL query implementation and its comparison with traditional tools are given in (Burdakov et al., 2019). Paragraph 3 develops a cost model of query execution processes. It can be represented in the form of nested structures with a "star" scheme (Fig. 6). Paragraph 4 shows the results of model calibration and its adequacy assessment with the Q3, Q17 queries and their stages.

2 REPRESENTATION OF AN ORIGINAL QUERY WITH SUBSEQUENT SUB-QUERIES

Let us start with examples for an original query transformation into a sequence *S* of sub-queries $\{Z_i\}$ and their execution results join $\{J_i\}$.

Example 1: Fig. 1 shows the Q3 query from the TPC-H test (TPC, 2019).

The Q3 query execution schema is shown in Fig. 2. Each box Z_i provides a source table identifier along with a filter condition shown in round brackets.

```
select l_orderkey, sum(l_extendedprice*(1-l_discount)) as revenue,
o_orderdate, o_shippriority
from customer, orders, lineitem
where c_mktsegment = '[SEGMENT]' and c_custkey = o_custkey
      and l_orderkey = o_orderkey and o_orderdate < date '[DATE]'
      and l_shipdate > date '[DATE]'
group by l_orderkey, o_orderdate, o_shippriority
order by revenue desc, o_orderdate;
```

Figure 1: Q3 query from TPC-H test.

The following TPC-H source table identifiers are provided: D_1 – customer, F_1 – orders, F_2 – lineitem.

Fig. 2 has two join stars: Z_1, Z_2 - J_1, and J_1, Z3 - J_2. Each star has one dimension and one fact table (separated with a comma). The join result in the first star (J_1) becomes a dimension in the second star.

Fig. 2 shows that each star can have a Bloom filter applied (Bloom, 1970; Tarkoma, 2012). Bloom filter is generated at the creation of a dimension table (see Fig. 2). During the fact table creation (usually large) its records are additionally filtered with that Bloom filter (see squares in Fig. 2). This significantly reduces the volume of data transmitted over the network at the shuffle phase and cuts the table join time at the Reduce phase (Burdakov et al., 2019).

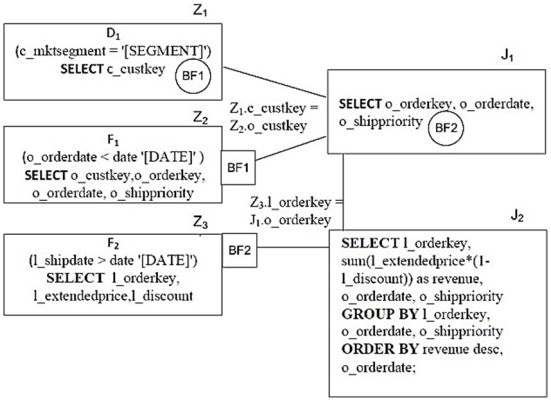

Figure 2: Q3 query execution schema.

Example 2: Fig. 3 shows Q17 query with a correlated sub-query from TPC-H test.

Please, note that Spark SQL cannot execute this query in its original form. It has to be decomposed into sub-queries. Fig. 4 presents the Q17 query execution schema. The following identifiers denote the source tables from the TPC-H database schema: D_1 – part, F_1 – lineitem.

```
select sum(l_extendedprice)/7.0 as avg_yearly from lineitem, part
where p_partkey = l_partkey and p_brand = '[BRAND]'
      and p_container = '[CONTAINER]' and l_quantity < (
select 0.2 * avg(l_quantity) from lineitem where
      l_partkey = p_partkey );
```

Figure 3: Q17 query from TPC-H test.

We can identify here the following two stars: Z_1, Z_2-J_1, and J_1, Z_3 - J_2.

Each star has an enabled Bloom filter. Fig. 4 shows that for the first star a broadcast distribution is executed for a small dimension table Z_1 (see diamond) over the nodes that store fact table Z_2(BF1) fragments. There Z_1 and Z_2(BF1) tables join is performed in RAM at the Map stage (w/o shuffle and w/o Reduce task execution).

Let us call the structure depicted in Fig. 2 and Fig. 4 as a *query structure*. Representation of the source queries in the form of stars allows describing the source query as a Z_i sequence of sub-queries and J_j joins, and connecting Bloom filter or executing a

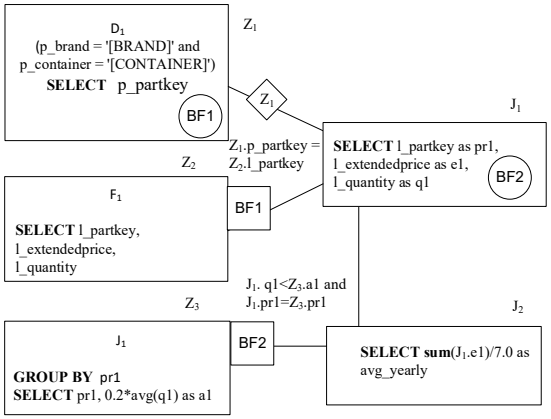

Figure 4: Q17 query execution schema.

broadcast distribution of small dimension tables. This can be done for almost any SQL query. To do this, all "select" queries have to be represented in intermediate tables and include them into the "from" clause of the original query. Table 1 provides the intermediate tables composition schemas for various SQL "select" sub-queries (Date et al., 1993). The corresponding TPC-H test query names are shown in round brackets. DataFrame/DataSet can implement intermediate tables in Spark.

Table 1: Intermediate table composition schemas.

SQL "select" sub-queries	Intermediate table composition schema
Sub-query is in the "from" clause of the original query (Q7, Q8, Q9, Q13).	Represent the sub-query in the form of a new table after the "from" clause of the original query.
Non-correlated sub-query (Q11, Q15, Q16, Q18, Q20, Q22).	Represent the sub-query in a form of a scalar (aggregate, EXISTS, NOT EXISTS) or table with one column; use table with IN, NOT IN, and use scalar in comparison operations of the original query.
Correlated sub-query (Q2, Q4, Q17, Q20, Q21, Q22).	Add required attributes from the original query into sub-query, perform group by; represent the sub-query in a table form; add table name into "from" of the original query; replace condition with a sub-query after "where" of the original query with a condition with required comparison operations.

The steps described in Table 1 are recursive. A "select" sub-query can be treated as an original query.

To generate an original query execution program, a query schema shall be built (please, see Fig. 2 and 4). The following language operator generation algorithm shall be applied in the next step (Fig. 5).

Fig. 5 has the following elements:

J_j^r - j-th join (as a dimension) in the r-th three of the query schema, $J_j^r \in \{J_1, \dots, J_{NJ}\}$,

Z_j^r - j-th sub-query (as a dimension) in the r-th star of the query schema, $Z_j^r \in \{Z_1, \dots, Z_{NZ}\}$.

```
main:
 star(J_NJ);
    delete join {J_i} and sub-query {Z_i} duplicates (if any);
duplicates will exist if the same joins or sub-queries are
used as sub-queries in a few stars;
    end main;
star (J):
 r: J == J_r
 CYCLE on j
  star(J_j^r)
 END OF CYCLE
 CYCLE on j
  Select statement for sub-query Z_j^r
 [Bloom filter create or apply operators]
 END OF CYCLE
 Select statement for J_r join
 [Bloom filter creation operators]
end star;
```

Figure 5: Program generation algorithm for source code execution in Spark.

Each star has one dimension table and one fact table in the provided examples 1 and 2. One can derive from the algorithm shown in Fig. 5 that each J_r join corresponds to a star with a join of a few dimension tables $\{D_i\}$ and fact table F (cycle on j). This is true for the "snowflake" query schema.

Fig. 6 shows dfD_i sub-queries implementation schema of the original query star and their join with the F fact table.

The transformation and action sequence (see Fig. 6) forms DAG (Directed Acyclic Graph) for the star implementation. It works like a conveyor processing df fragments in parallel through the graph nodes (the fragments stored on the cluster nodes). This is a plan for the "star" schema (D_1,..., D_n – F), which can be used as a dimension in another star. The partition processing track is provided below (stages 1-4):

1. Read Di dimension tables, filter records with the Pi condition, obtain the projection (ki, wi).

2. Build Bloom filters for dfDi table partitions in RAM (by ki key for each dimension), assemble each Bloom filter in a Driver (logical OR) followed by broadcast distribution of the Bloom filter to all Executors which perform fact table filtration (F).

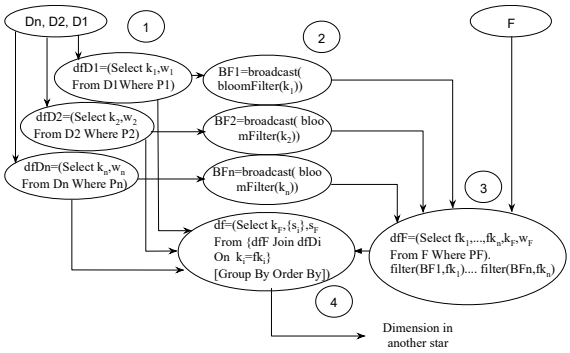

Figure 6: Original query star implementation general schema.

3. Read fact table, filter records with PF condition and with Bloom filters, obtain projection ({fk_i}, k_F, w_F).

4. Join the filtered fact table with the filtered dimension tables (dfF Join dfD_i). Group and sort if applicable to the particular "star" schema. Jump to a new star in the query schema.

3 COST MODEL DEVELOPMENT

A cost model has the following features (Leis et al., 2015):

1. Uniform distribution: it is assumed that all values of an attribute are uniformly distributed in a given interval.
2. Independence: attribute values are considered independent (whether in the same table or different tables).
3. Inclusion principle: join key domains overlap in a way that the smaller domain's keys are present in the larger domain.

A dataset that adheres to features 1-3 is called synthetic, e.g. TPC-H database is synthetic.

Spark creates one or a few parallel processes at each stage. Fig. 7 demonstrates an example.

The lines in Fig. 7 denote process intervals (the beginning and the end). The duration of the intervals (t_{ix}), i.e. resource consumption time, is shown above the lines. We will consider the average values. A process can create another process (at the end of t_{ix}). For example, the chain of created processes for node 1 looks as follows: $P_{1D} \rightarrow P_{1P} \rightarrow P_{1B}$. The Fig. 7 shows that two processes with the same name executed on different nodes (or on different processor cores of the same node) form a group of parallel similar processes (PSP). The following three groups can be identified: (P_{1D}, P_{2D}), (P_{1P}, P_{2P}), (P_{1B}, P_{2B}).

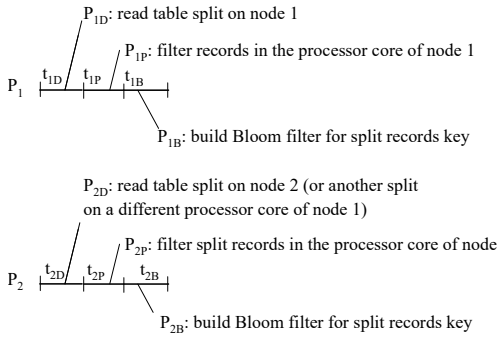

Figure 7: Spark-created Processes Example.

Let us denote the PSP group with a line corresponding to the group interval definition (see Fig. 8). The parent PSP creates descendant PSPs, e.g. descendant PSP P_P is created by parent PSP P_D and so on. Let us call a PSP groups set as *connected parallel processes* (CPP). For example, P_D, P_P, P_B PSPs form CPP with P identifier (see Fig. 8).

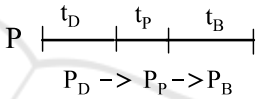

P_D - read split on a node

P_P - filter split records in processor core of a node

P_B - build Bloom filter for split records

Figure 8: PSP Group (P_D, P_P, P_B) and CPP (P) Notation.

Let us represent CPP for simplicity with one line that corresponds to a *CPP interval*. The interval duration is equal to the duration between the beginning and the end of all activities of the PSP included in the set. Let us call it the duration for the execution of connected parallel processes. Each CPP interval will be provided with an identifier (e.g. P in Fig. 8). CPP instance frequently corresponds to a task that is executed in the Executor slot.

Based on the Spark processes analysis (see Fig. 6) we developed a mathematical model. Fig. 9 provides a process execution description for sub-queries and joins related to one star of the original query. The lines in Fig. 9 correspond to a CPP:

1. R_i CPP. Reading and processing of dimension tables, creation of Bloom filters for a key (BFi=bloomfilter(k_i)).
2. A CPP. Assembly of the Bloom filters in the Driver program, OR join, broadcast distribution throughout the nodes.
3. R_F CPP. Reading and processing of fact tables, record filtration with the Bloom filter (fk_i is the foreign key of the fact table).

A "group by" operation for a fact table sometimes precedes Bloom filter application.

The items 4 and 5 are then executed if L>0 (L is the number of small tables).

4. B CPP. Broadcast distribution of filtered dimension tables which size does not exceed the V_M threshold.

5. C CPP. Hash Join of fact table with 1…L dimension tables in RAM.

Items 6 and 7 are executed further if L<n.

6. X_i (i=1…n-L+1) CPP. Sorting on the Map side of each dimension table partition (dfD_{L+1}...dfD_n) or fact table (dfFH) by the join key, storage of the sorted partitions in the local file system (Shuffle Write).

7. Y_i (i=1…n-L) CPP. Pairwise join of the fact and dimension tables.

If the original query has a "group by" (Z_1) or "order by" (Z_2) parts then items 8 and 9 are also executed.

8. Z_1 CPP. Grouping at the end of the query execution.

If there is order by part then item 9 is also executed.

9. Z_2 CPP. Sorting at the end of the query execution.

The table obtained as the result of the sub-queries execution and star joins of the original query can serve as a dimension in the next star.

The original query execution time is estimated as a sum of CPP intervals 1-9 of all stars.

The limited volume of the paper does not allow providing all formulas for calculation of CPP 1-9 intervals. Let us provide formulas for R_i CPP interval calculation. The formulas (1)-(7) use the following elements:

N – cluster nodes (workers) number; NC – total CPU quantity in a cluster (the number of Executor slots, quantity of physical cores); V_S – split block size (bytes); V_{Di}, Q_{Di} – compressed volume and the number of records in the i-th dimension table (i=1…n); P_i - probability that a record satisfies the search condition for the i-th dimension table; μ_{RH} - data read intensity from HDFS file system (byte/sec); τ_d – processor time for task deserialization in Executor slot; τ_f – processor time for filtration per record; τ_b – processor time for record read/write from Bloom filter.

The number of slots (tasks) required to process the i-th dimension table is equal to:

$$N_{Si} = \lceil V_{Di}/V_S \rceil . \quad (1)$$

The following formula gives the records number per slot:

$$Q_{Si} = Q_{Di}/N_{Si} . \quad (2)$$

Split volume for the i-th dimension table equals to:

$$V_{Si} = \begin{cases} V_S, if\ N_{Si} \geq 2, \\ V_{Di}, if\ N_{Si} = 1 \end{cases} \quad (3)$$

Let us calculate one task execution time connected to record processing in the i-th dimension table:

$$r_i = \tau_d + V_{Si}/\mu_{RH} + \tau_f Q_{Si} + \tau_b P_i Q_{Si}. \quad (4)$$

The Executor slot may be consequentially processing a few tasks. Let a task related to the m-th dimension table be planned for a slot:

$$m: r_m = max\{r_i\} . \quad (5)$$

The split blocks of the table are distributed over the cluster nodes uniformly. Hence the probability that the same slot would get the rest of the dimension table tasks planned where each task processes one table split equals to:

$$\frac{1}{N} \cdot \frac{1}{NC/N} = \frac{1}{NC} . \quad (6)$$

The dimension tables processing time will be equal to:

$$r = r_m + \frac{N_{Sm}-1}{NC} r_m + \sum_{\substack{i=1 \\ i \neq m}}^{n} \frac{N_{Si}}{NC} r_i = (1 - \frac{1}{NC}) r_m + \frac{1}{NC} \sum_{i=1}^{n} N_{Si} r_i . \quad (7)$$

4 MODEL CALIBRATION AND ADEQUACY EVALUATION

The mathematical model of the processes shown in Fig. 9 was implemented in Python. A test stand that included a virtual cluster was used to calibrate the model. The cluster had 8 nodes with HDFS, Hive, Spark, Yarn (Vavilapalli et al., 2013). Each node had a double core processor, 200 GB SSD disk, Ubuntu 14.16 OS. The results of the experiments were split into two subsets.

The first subset had execution of ten queries: five Q3 queries with SF=500 (NBF=40 million), SF=250 (NBF=50 million), SF=100, SF=50, SF=10 (NBF=15 million) database population parameters, where SF is the scale factor for database size of TPC-H (TPC, 2019), NBF – anticipated number of element in BF1 and BF2 Bloom filters; and five Q17 queries with SF=500, SF=250, SF=100, SF=50, SF=10 (NBF=15 million).

The corresponding query execution time (10 points) was used to calibrate model parameters with the Least Squares Method (LSM) with gradient descent. Table 2 provides the calibrated parameters of the model, their variation ranges and optimal values.

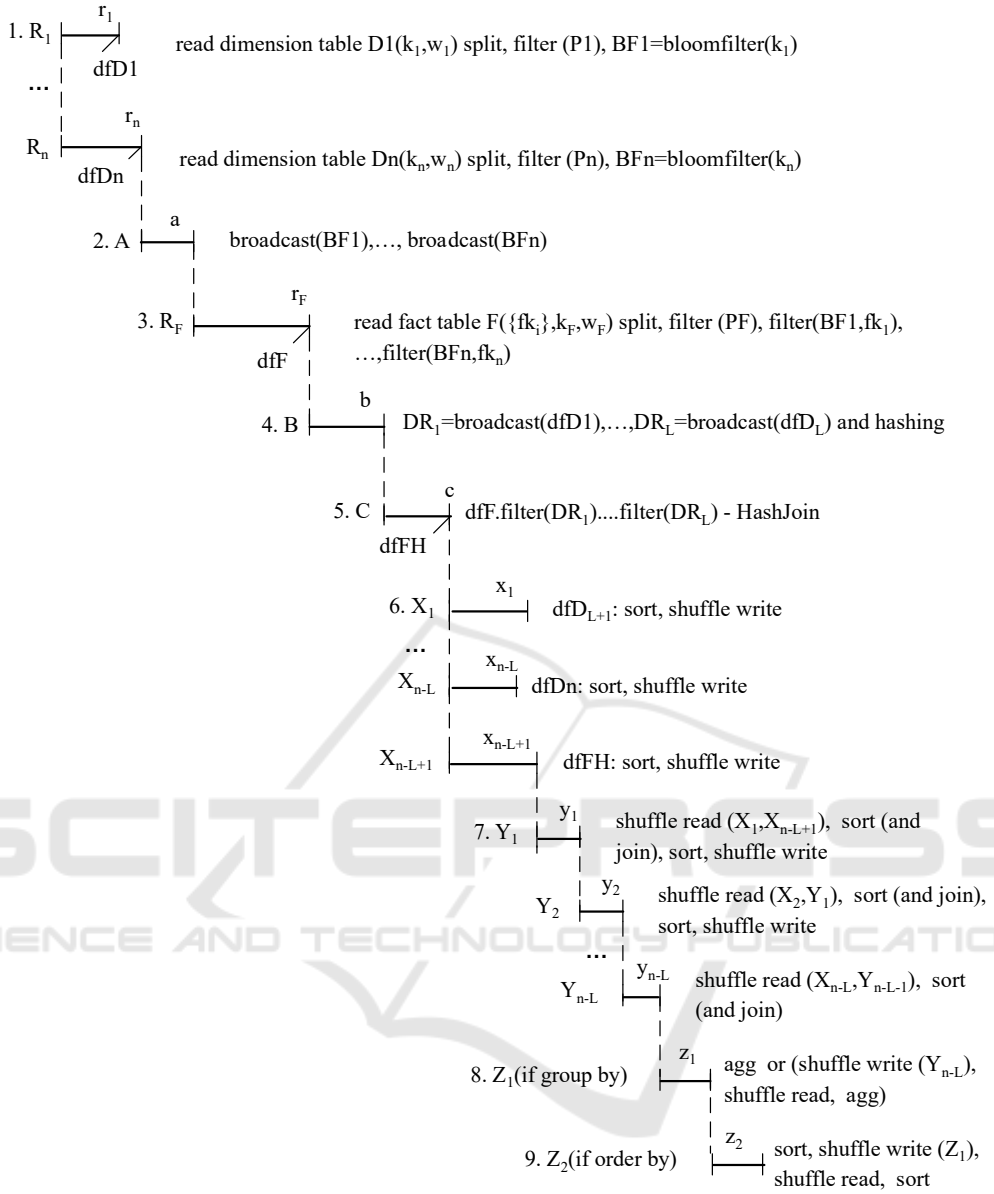

Figure 9: Implementation processes description for sub-queries and joins correspondent to the original query star.

The optimal values for the calibrated model parameters were found in the following way: the outer cycle randomly selected a point inside 9-dimensional parallelepiped (9 is the number of calibrated parameters), while the inner cycle performed error minimization by numerical methods with gradient descent. The error function equals the sum of squared differences between the execution times of ten experimental and modelled queries. Since the error function may have multiple minimums and there is a possibility of going beyond the ranges, the outer cycle was repeated 100 times.

The sum of squared deviations of modelled time from the experiment measurements equalled to 27079 for 10 queries.

We developed a universal interface allowing setting up and calibrating an arbitrary model.

The second subset of experimental results had query execution time for 40 query stages: stages 0,1,2,3,6,7,8 of Q3 query with SF=500 (NBF=40 million), SF=250 (NBF=50 million), SF=100, SF=50, SF=10 (NBF=15 million) database population parameters; and stages 0, 2, (3+5), 4, (6+7) of Q17 query with SF=500 (NBF=15 million) database population parameters.

Stages execution time (40 measurements) were used for model adequacy evaluation.

Table 2: Model Calibration Parameters and their Optimal Values.

Calibrated Model Parameter	Lower Limit	Upper Limit	Optimal Value
τ_f – processor time of filtration per record, s	1.0E-06	1.0E-05	1.14E-06
τ_b – processor time for record read/write from Bloom filter, s	1.0E-08	1.0E-07	2.07E-08
τ_s – record sorting time per records, s	1.0E-08	1.0E-07	2.11E-08
τ_d – deserialization processor time for a task in the Executor slot, s	1.0E-06	1.0E-04	7.59E-05
τ_h – hashing time per record (for further comparison and aggregation), s	1.0E-08	1.0E-06	4.27E-07
KS – coefficient correspondent to serialization effect on the transmitted data volume during shuffle execution	0.5	1.5	0.81
μ_{RH} - HDFS file system data read intensity (MBps)	20.0	50.0	44.1
μ_{WL} - LFS local file system data write intensity (MBps)	50.0	200	61.4
μ_{N1} – network switch data transmission intensity (MBps)	100	500	186

A model vs. experiment scatter plot in Fig. 10 (50 points) shows all modeling and experimental query and their stages execution time from the two subsets.

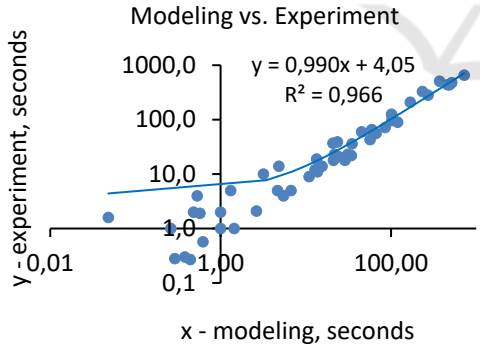

Figure 10: Query and stage modeling execution time (x) vs. experimental measurements (y).

The logarithmic scale is used for both axes: x1=lg x, y1=lg y. The regression dependency between y and x is expressed as y=0.99x+4.0≈x+4. For the logarithmic scale, it will be y1=lg(10^{x1}+4). For a large enough x1, we get y1=x1 and hence y=x. For x1→-∞ y1→ lg 4 (horizontal asymptote in Fig. 10). The coefficient of determination for the experimental data approximation of the regression is close to 1 (R^2=0.966), which shows a very high modelling accuracy for large modelling time values (y=x in this case). Fig. 10 demonstrates that for the values over 10 seconds the modelling accuracy is good (the dots are close to the y=x line). The relative modelling error ($\Delta=100\cdot|T_{Experiment}-T_{Modeling}|\div T_{Experiment}$) for points to right of x=10 (31 point) has the following distribution: 35% points have error $\Delta\leq10\%$, 19% points have $10\%<\Delta\leq20\%$, 23% points - $20\%<\Delta\leq30\%$, 13% points - $30\%<\Delta\leq40\%$ -, and 10% points - $\Delta>40$ %.

Fig. 10 shows that model parameters calibration allows building a good prognostic cost model for query execution time estimation for large databases even with non-precise cardinality values of intermediate tables (cardinality values are estimated on probability, P_i in formula (4)). Further, we provide a theoretical justification for this finding.

5 MODEL ADEQUACY THEORETICAL EVALUATION FOR LARGE DATABASES

Let us represent the random time of the i-th query execution:

$$t_i = \sum_{j=1}^{J_i} \sum_{k=1}^{|R_j|} \xi_{ijk}, \quad (8)$$

here J_i is a number of tables taking part in the i-th query execution, $|R_j|$ is j-th table number of records, $\xi_{ijk} \geq 0$ is random time of k-th record processing from j-th table during execution of the i-th query.

Let us further for simplicity assume that the database is synthetic. Then we can derive from the synthetic dataset's characteristics 1-3 (see Paragraph III) that the probability distribution function (PDF) of a random variable ξ_{ijk} does not depend on κ, and the number of records in tables is proportional to SF factor (even for the intermediate tables produced by joins). The number of records resulting from some m and n table joins for the j-th table will be equal to:

$$\frac{SF|R_{m1}|\cdot SF|R_{n1}|}{max(SF\cdot I(R_{m1},a),SF\cdot I(R_{n1},a))} = SF\cdot\left|R_{j1}\right|, \quad (9)$$

here $|R_{z1}|$ is the records number in table z given SF=1, z∈(m,n,j), $I(R_{z1},a)$ – join attribute a cardinality (unique values count) R_{z1} table, z∈(m,n).

Formula (8) can be expressed in the following way:

$$t_i = \sum_{j=1}^{J_i} \sum_{k=1}^{SF|R_{j1}|} \xi_{ij}, \quad (10)$$

Based on characteristic 2 of the synthetic databases let us consider independence of the random variables ξ_{ij}. These variables are limited on both sides so that the conditions of the Lyapunov theorem are satisfied (Zukerman, 2019). Given numerous additives in (10), the t_i PDF will be close to the normal distribution. The mathematical expectation and variance of query execution time can be derived from (10) in the following form:

$$E(t_i) = SF \sum_{j=1}^{J_i} |R_{j1}| E(\xi_{ij}) = SF \cdot E_1(t_i), \quad (11)$$

$$Var(t_i) = SF \sum_{j=1}^{J_i} |R_{j1}| Var(\xi_{ij}) = F \cdot Var_1(t_i), \quad (12)$$

here $E_1(t_i)$ and $Var_1(t_i)$ are mathematical expectation and variance of query execution time for SF=1.

The confidence interval for an arbitrary query execution time *t* can be calculated with the following formula:

$$|t - E(t)| \leq k_\alpha \sqrt{Var(t)}, \quad (13)$$

here α is the confidence level (13), k_α - α quantile: 0.95 quantile = 1.645, 0.99 quantile = 2.326, 0.999 quantile = 3.090.

From (11), (12), (13) we derive:

$$E(t)\left(1 - \frac{k_\alpha \sqrt{Var_1(t)}}{E_1(t)\sqrt{SF}}\right) \leq t \leq E(t)\left(1 + \frac{k_\alpha \sqrt{Var_1(t)}}{E_1(t)\sqrt{SF}}\right), \quad (14)$$

An arbitrary query set is used for model calibration so that the regression formula obtained with the Least Squares Method (LSM) is: $E(t)=y=x+c_1$, here x is modelling value, c_1 is some constant. If time *t* has Normal Distribution then LSM and MLE (maximum likelihood estimation) give the same result (Seber el al., 2012).

From (14) we derive:

$$x\left(1 + \frac{c_1}{x}\right)\left(1 - \frac{c_2}{\sqrt{SF}}\right) \leq t \leq x\left(1 + \frac{c_1}{x}\right)\left(1 + \frac{c_2}{\sqrt{SF}}\right), \quad (15)$$

here $c_2 = max_t \left(k_\alpha \sqrt{Var_1(t)} / E_1(t)\right)$.

Provided SF and *x* are large we derive from (15) that query execution time *t* corresponds well with the modelling value *x*. This confirms the distribution of the "experiment vs. model" points in Fig. 10.

Real datasets have many correlations and uneven data distribution. The developed model though should not lose its adequacy with the real data. Query execution time (8) has Normal Distribution even if ξ_{ijk} random variables correlate in case the maximum correlation coefficient tends to 0 as the distance between elements increases (Seber et al., 2012). We can relax the uniform distribution requirement for data and use $SF = min_i \sum_{j=1}^{J_i} |R_j|$, which is determined by the data stored in a database.

The overall point distribution in Fig. 10 corresponds to the results described in (Leis et al., 2015) for query execution in the real database (please, see, the left column in Fig. 8 in (Leis et al., 2015)). Please note that these diagrams were plotted for non-calibrated cost models.

6 CONCLUSION

We developed a mathematical model for Spark processes based on the sub-models of connected parallel processes (Fig. 9). The model can help to predict SQL query execution time based on its schema. Fig. 2 and Fig. 4 provide schema construction examples, and Table 1 shows how to do it for other queries.

Based on the experimental results (overall 50 points) the model parameters were calibrated and its adequacy evaluated. The coefficient of determination for linear regression approximation is R^2=0.966, which shows good model accuracy for high modelling time values. It was shown that for modelling time over 10 seconds the points are concentrated close to the y=x line (Fig. 10). 77% of these points have relative modelling error Δ<30%. This is satisfactory for predicting query execution time in a distributed parallel system which requires time estimation, e.g. for a DaaS environment, or performs comparison and selection of query implementation option, i.e. for query optimization.
The model gives an acceptable accuracy even with non-precise intermediate table cardinalities. This is important since unlike with relational databases calculation of the precise cardinality in a distributed environment requires complete table analysis.

REFERENCES

Akdere, M. et al. (2012) Learning-based query performance modeling and prediction //Data Engineering (ICDE), 2012 IEEE 28th International Conference on. – IEEE, 2012. – pp. 390-401.

Armbrust M. et al. (2015) Spark SQL: Relational data processing in spark //Proceedings of the 2015 ACM SIGMOD international conference on management of data. – ACM, 2015. – pp. 1383-1394.

Bloom, B. H. (1970) Space/time trade-offs in hash coding with allowable errors // Communications of the ACM. – 1970. – Vol. 13. – №. 7. – Pages 422-426.

Burdakov, A., Ermakov, E., Panichkina, A., Ploutenko, A., Grigorev, U., Ermakov, O., & Proletarskaya, V. (2019). Bloom Filter Cascade Application to SQL Query Implementation on Spark. In 2019 27th Euromicro International Conference on Parallel, Distributed and Network-Based Processing (PDP) (pp. 187-192). IEEE

Chi, Y., Moon, H. J. and Hacigümüş, H. (2011) iCBS: incremental cost-based scheduling under piecewise linear SLAs //Proceedings of the VLDB Endowment. – 2011. – T. 4. – №. 9. – pp. 563-574.

Date, C. J., and Darwen, H. (1993). A Guide to the SQL Standard (Vol. 3). Reading: Addison-wesley.

Dean, J. and Ghemawat, S. (2004) MapReduce: Simplified data processing on large clusters. In Proceedings of the Sixth Conference on Operating System Design and Implementation (Berkeley, CA, 2004).

Ganapathi, A. et al. (2009) Predicting multiple metrics for queries: Better decisions enabled by machine learning //Data Engineering, 2009. ICDE'09. IEEE 25th International Conference on. – IEEE, 2009. – pp. 592-603.

Guirguis, S. et al. (2009) Adaptive scheduling of web transactions //Data Engineering, 2009. ICDE'09. IEEE 25th International Conference on. – IEEE, 2009. – pp. 357-368.

Mishra, C. and Koudas, N. (2009) The design of a query monitoring system //ACM Transactions on Database Systems (TODS). – 2009. – T. 34. – №. 1.

Leis, V. et al. (2015) How good are query optimizers, really? //Proceedings of the VLDB Endowment. – 2015. – T. 9. – №. 3. – pp. 204-215.

Mistrík, I., Bahsoon, R., Ali, N., Heisel, M., & Maxim, B. (Eds.). (2017). Software Architecture for Big Data and the Cloud. Morgan Kaufmann.

Odersky, M., Spoon, L., & Venners, B. (2008). Programming in scala. Artima Inc.

Seber, G. A., and Lee, A. J. (2012). Linear regression analysis (Vol. 329). John Wiley & Sons.

Tarkoma, S., Rothenberg, C. and Lagerspetz, E. (2012) "Theory and practice of bloom filters for distributed systems" IEEE Comms. Surveys and Tutorials, vol. 14, no. 1, pp. 131–155, 2012.

Tozer, S., Brecht, T. and Aboulnaga, A. (2010) Q-Cop: Avoiding bad query mixes to minimize client timeouts under heavy loads //Data Engineering (ICDE), 2010 IEEE 26th International Conference on. – IEEE, 2010. – pp. 397-408.

TPC org. (2019) "Documentation on TPC-H performance tests", tpc.org. [Online]. Available: http://www.tpc.org/tpc_documents_current_versions/pdf/tpc-h_v2.17.2.pdf. [Accessed: Sept. 22, 2019]

Vavilapalli, V.K., et al. (2013) "Apache hadoop yarn: Yet another resource negotiator." Proceedings of the 4th annual Symposium on Cloud Computing. ACM, 2013, p. 5

Wasserman, T. J. et al. (2004) Developing a characterization of business intelligence workloads for sizing new database systems //Proceedings of the 7th ACM International Workshop on Data Warehousing and OLAP. – ACM, 2004. – pp. 7-13.

Wu, W. et al. (2013) Predicting query execution time: Are optimizer cost models really unusable? //Data Engineering (ICDE), 2013 IEEE 29th International Conference on. – IEEE, 2013. – pp. 1081-1092.

Xiong, P. et al. (2011) ActiveSLA: a profit-oriented admission control framework for database-as-a-service providers //Proceedings of the 2nd ACM Symposium on Cloud Computing. – ACM, 2011. – P. 15.

Zukerman, M. (2019) Introduction to Queueing Theory and Stochastic Teletrac Models. [Online]. Available: http://www.ee.cityu.edu.hk/~zukerman/classnotes.pdf. [Accessed: Sept. 22, 2019].

SCITEPRESS SCIENCE AND TECHNOLOGY PUBLICATIONS